THE ASTRONOMICAL JOURNAL VOLUME 105, NUMBER 6 JUNE 1993

PHOTOMETRIC AND SPECTROSCOPIC OBSERVATIONS OF SN 1990E IN NGC 1035: OBSERVATIONAL CONSTRAINTS FOR MODELS OF TYPE II SUPERNOVAE[1]

BRIAN P. SCHMIDT, ROBERT P. KIRSHNER,[2] RUDY SCHILD, BRUNO LEIBUNDGUT,[3] DAVID JEFFERY, S. P. WILLNER, REYNIER PELETIER, AND ANN I. ZABLUDOFF

Harvard-Smithsonian Center for Astrophysics, 60 Garden St., Cambridge, Massachusetts 02138
Electronic mail: brian@cfanewton.harvard.edu, kirshner@cfanewton.harvard.edu, bruno@popsicle.berkeley.edu, jeffery@cfanewton.harvard.edu, willner@cfa.harvard.edu, zabludof@cfa

MARK M. PHILLIPS, NICHOLAS B. SUNTZEFF, MARIO HAMUY, LISA A. WELLS, R. CHRIS SMITH, JACK A. BALDWIN, W. G. WELLER, M. NAVARETTE, AND L. GONZALEZ

Cerro Tololo Inter-American Observatory,[4] Casilla 603, La Serena, Chile
Electronic mail: mphillips@ctio.noao.edu, nsuntzeff@ctio.noao.edu, mhamuy@ctio.noao.edu, lwells@noao.edu, csmith@ctio.noao.edu, jbaldwin@ctio.noao.edu

ALEXEI V. FILIPPENKO,[5] JOSEPH C. SHIELDS,[6] AND CHARLES C. STEIDEL

Department of Astronomy and Center for Particle Astrophysics, University of California, Berkeley, California 94720
Electronic mail: alex@bkyast.berkeley.edu

SAUL PERLMUTTER, CARLTON PENNYPACKER, AND CRAIG K. SMITH

Lawrence-Berkeley Laboratory, University of California, Berkeley, Berkeley, California 94720
Electronic mail: pennypacker@lbl.gov, saul@lbl.gov., csmith@csa2.lbl.gov

ALAIN C. PORTER AND TODD A. BOROSON

Kitt Peak National Observatory,[4] P.O. Box 26732, Tucson, Arizona 86726
Electronic mail: aporter@noao.edu, tborason@noao.edu

RAYLEE STATHAKIS AND RUSSELL CANNON

Anglo-Australian Observatory, Epping Laboratory, P.O. Box 296, Epping, N.S.W. 2121 Australia
Electronic mail: rl@aaoepp.oz.au

J. PETERS AND E. HORINE

F. L. Whipple Observatory, Box 97, Amado, Arizona 85721

KENNETH C. FREEMAN

Mt. Stromlo and Siding Spring Observatory, Private Bag, Woden PO, 2606 Canberra, ACT, Australia
Electronic mail: kcf@merlin.anu.oz.au

DONNA S. WOMBLE

Center for Astrophysics and Space Sciences, University of California, San Diego, 9500 Gillman Dr., La Jolla, California 92093-0111
Electronic mail: dwomble@ucsd.edu

REMINGTON P. S. STONE

Lick Observatory, University of California, Santa Cruz, California 95064
Electronic mail: rem@ucscloc.ucsc.edu

LAURENCE A. MARSCHALL[2]

Department of Physics, Gettysburg College, Gettysburg, Pennsylvania 17325
Electronic mail: marschall@gettysburg.edu

ANDREW C. PHILLIPS[7]

Department of Astronomy FM-20, University of Washington, Seattle, Washington 98195

A. SAHA[2] AND HOWARD E. BOND[7]

Space Telescope Science Institute, 3700 San Martin Dr., Baltimore, Maryland 21218
Electronic mail: saha@scivax.stsci.edu, bond@scivax.stsci.edu

Received 1992 December 14; revised 1993 January 29

 0004-6256/93/062236-15$00.90

ABSTRACT

We present 126 photometric and 30 spectral observations of SN 1990E spanning from 12 days before *B* maximum to 600 days past discovery. These observations show that SN 1990E was of type II-P, displaying hydrogen in its spectrum, and the characteristic plateau in its light curve. SN 1990E is one of the few SNe II which has been well observed before maximum light, and we present evidence that this SN was discovered very soon after its explosion. In the earliest spectra we identify, for the first time, several N II lines. We present a new technique for measuring extinction to SNe II based on the evolution of absorption lines, and use this method to estimate the extinction to SN 1990E, $A_V = 1.5 \pm 0.3$ mag. From our photometric data we have constructed a bolometric light curve for SN 1990E and show that, even at the earliest times, the bolometric luminosity was falling rapidly. We use the late-time bolometric light curve to show that SN 1990E trapped a majority of the gamma rays produced by the radioactive decay of ^{56}Co, and estimate that SN 1990E ejected $0.073^{+0.018}_{-0.051}$ $\mathcal{M}_\odot$ of ^{56}Ni, an amount virtually identical to that of SN 1987A.

1. INTRODUCTION

On 1990 February 15.1, (UT), the Berkeley Automated Supernova Search Team (BASST; Perlmutter *et al.* 1988) observed NGC 1035 and detected a new star at the edge of this highly inclined Sc galaxy (Pennypacker & Perlmutter 1990). This object was especially interesting because it had not been detected in a similar observation just five days earlier. An intense effort was made to gather spectroscopic data after discovery; these spectra revealed a weak P-Cygni feature at Hα indicating that the new supernova, SN 1990E, was a very young type II. Programs at Cerro Tololo Inter-American Observatory (CTIO) and Fred Lawrence Whipple Observatory (FLWO) were initiated to obtain spectra and photometry on a regular basis, and additional observations were made at observatories around the world. This paper reports these observations and uses them to discuss the properties of the explosion. Unfortunately, despite the early discovery, SN 1990E could be observed for only one month before it disappeared into the evening twilight. Our observations of SN 1990E resumed 90 days later and continued for another 400 days.

The photometric (Young & Branch 1989; Kirshner 1990) and spectroscopic (Branch 1990) variation of type II supernovae is well documented. SNe II have been subdivided into two groups based on the shapes of their light curves (Barbon *et al.* 1979): SNe II-L(inear), after maximum, exhibit an exponential decline (linear in magnitudes), whereas SNe II-P(lateau) maintain a more or less constant brightness for approximately 100 days past maximum. Our data show SN 1990E is a typical SN II-P, although the plateau phase was not directly observed due to the gap in observing as the SN passed behind the sun.

SN 1987A, which is closely related to the SN II-P despite a unique light curve, has furthered our understanding of this class of supernovae enormously. SN 1987A arose from the explosion of a blue supergiant (Arnett *et al.* 1989); typical SNe II-P, such as SN 1990E, are thought to have red supergiants as their progenitors. Although the physics of the core collapse, neutrino transport, and nucleosynthesis in supernovae do not depend on the extent of the atmosphere, SNe arising from blue supergiants have significant differences in their spectra and light curves relative to SNe with extended progenitors (Woosley *et al.* 1987). Our extensive data set for SN 1990E includes photometry from which the temperature and the energy output of the supernova can be measured, and spectra which provide clues to the temperature, density and velocity structure, and chemical composition of SN 1990E's atmosphere. These data constrain explosion models of SNe II-P and provide the information needed to model accurately the atmosphere of SN 1990E (Eastman *et al.* 1993). Information from these model atmosphere calculations, when input into the expanding photosphere method, provides a distance to the SN which is completely independent of the cosmic distance ladder (Schmidt *et al.* 1992).

2. OBSERVATIONS

The optical flux from SN 1990E was followed for nearly 600 days using CCD imaging systems on the CTIO 4 m, CTIO 0.9 m, KPNO 2.1 m, KPNO 0.9 m, and FLWO 0.61 m telescopes. The CCD images were bias subtracted and

[1]Work based in part on observations at the Multiple Mirror Telescope, a joint facility of the Smithsonian Astrophysical Observatory and the University of Arizona.

[2]Visiting Astronomer, Kitt Peak National Observatory, National Optical Astronomy Observatories, operated by the Association of Universities for Research in Astronomy, Inc. (AURA), under cooperative agreement with the National Science Foundation.

[3]Present Address: Department of Astronomy, University of California, Berkeley, CA 94720.

[4]Operated by the Association of Universities for Research in Astronomy, Inc. (AURA), under cooperative agreement with the National Science Foundation.

[5]Presidential Young Investigator.

[6]Present Address: Department of Astronomy, Ohio State University, 174 W. 18th Avenue, Columbus, OH 43210.

[7]Visiting Astronomer, Cerro Tololo Inter-American Observatory, National Optical Astronomy Observatories, operated by the Association of Universities for Research in Astronomy, Inc. (AURA), under cooperative agreement with the National Science Foundation.

TABLE 1. Magnitudes of comparison stars.

Star	B	V	R	I	J	H
1	14.77 ± .01	14.21 ± .01	13.89 ± .03	13.54 ± .03	13.44 ± .10	13.10 ± .10
2	18.93 ± .04	18.00 ± .03	17.43 ± .03	16.94 ± .03	—	—
3	18.62 ± .04	17.74 ± .03	17.22 ± .03	16.74 ± .05	—	—
4	22.75 ± .10	21.39 ± .10	20.19 ± .07	18.48 ± .08	—	—
5	22.35 ± .10	21.23 ± .10	20.75 ± .09	19.95 ± .08	—	—

flatfielded in the usual manner. On nine photometric nights at CTIO and KPNO, Landolt (1992) and Graham (1982) standard star fields were observed frequently throughout the night to determine transformation coefficients to the standard systems of Johnson (Johnson *et al.* 1966; for *BV*) and Cousins (Cousins 1980, 1981; for *RI*). Instrumental magnitudes for the standard stars were measured using the IRAF "PHOT" package. First-order transformation coefficients were calculated using the procedure described in Harris *et al.* (1981); in particular, the color terms were solved simultaneously for nights which had the same instrumental configuration. The derived transformation coefficients were used to calibrate a sequence of five stars near SN 1990E [Fig. 1 (Plate 104)]. The magnitudes of these five stars were determined from the mean of the observations, and the associated error estimates were derived from the mean error, as listed in Table 1. Stars 4 and 5, which were particularly faint, were chosen because the CCD imaging system used on the KPNO 2.1 m has a very small field, and these were the only usable reference stars.

Measuring the brightness of SN 1990E is complicated by the background surface brightness of the host galaxy ($m_R \approx 20$ mag/arcsec^2 at the position of the SN). We use DOPHOT (Mateo & Schechter 1989) to perform relative photometry between the comparison stars and the supernova. DOPHOT approximates the point spread function (PSF) for objects in an image to be Gaussian. The parameters for this analytic PSF are derived from all stars in an image that are brighter than a threshold. By varying the brightness of an object and the background until a best fit to the PSF is obtained, DOPHOT estimates the brightness of the object and the underlying background. We check the accuracy of photometry using this method by placing artificial stars on an image of NGC 1035 taken after SN 1990E had faded away. We find that DOPHOT can systematically overestimate or underestimate the brightness of an object when there is a strong gradient in the background. These systematic errors are reduced substantially by using only the inner core (1.5 times the FWHM) of an object to fit the PSF, and this is the procedure we have adopted. The power of DOPHOT is demonstrated in Fig. 2, where we compare photometry of artificial stars using DOPHOT and apertures. For the aperture photometry, we determine the background from images on which synthetic PSFs were not placed. DOPHOT produces photometry which is substantially more accurate than apertures on objects which are superimposed on complex backgrounds. DOPHOT also has the advantage that it does not require waiting for the SN to fade from view so that a separate measurement of the background brightness can be made. Filippenko *et al.* (1986) show that accurate photometry can be obtained of a SN lying in a complex region by subtracting an image

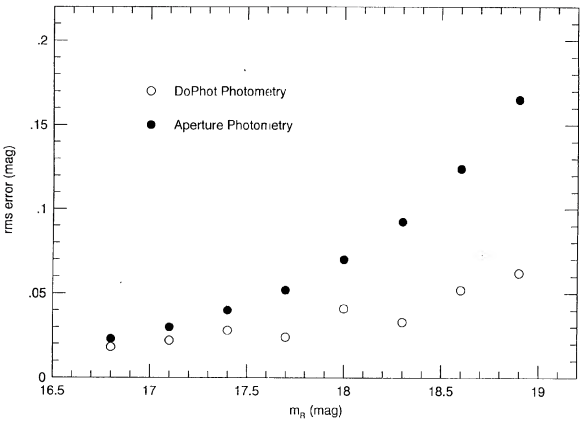

FIG. 2. Comparison of photometry obtained using DOPHOT and apertures of synthetic stars placed on to NGC 1035. The image used for this analysis was a 10 min exposure taken in *R* with the KPNO 2.1 m in 0.8″ (FWHM) seeing. For the aperture photometry, the background was determined from an image taken a year later with the same CCD and filter combination.

taken when the SN is no longer visible from the images where the SN is detected. This method is difficult and time consuming to implement. To subtract the galaxy background from the SN, the images to be differenced must be obtained with the same CCD and filter set. Furthermore, the images must be convolved to the same seeing, as well as rotated and shifted—a laborious process. *Except* in situations where spatial fluctuations in the host galaxy obscure the PSF of the SN (e.g., the SN occurs at the position of a compact H II region, or observations made at extremely late times), we believe that the gains of this more painstaking method over DOPHOT are small.

Corrections for differences in the color of the SN compared to the reference stars were made for epochs when the supernova's flux was dominated by the continuum (i.e., from discovery through March). These corrections are small because the SN is compared to Star 1 at early times, and at this time, the two objects have similar colors (Tables 1 and 2). No color corrections were made at later times because the flux of the SN was dominated by relatively narrow emission lines; this emission is completely different from that of stars on which the color corrections are based. Error estimates were made by adding the relative photometry and reference star brightness uncertainties in quadrature. The photometry of SN 1990E and the associated error estimates are given in Table 2. Additional photometric observations have been reported in the IAU circulars by Benetti *et al.* (1990), and they agree with ours to 0.10 mag where they overlap.

SN 1990E was not visible on an unfiltered CCD image of NGC 1035 (JD=2447932.6) taken by the BASST five days before discovery. We have observed Landolt (1983) standard stars using the BASST telescope and have determined that the unfiltered CCD used for these observations most closely resembles the *R* filter. By adding artificial PSFs to the image at the location of the SN, we are able to obtain an upper limit to the supernova's brightness at this

TABLE 2. Photometry of SN 1990E.

Date (UT)	JD (2440000+)	B	V	R	I	(B-V)	(V-R)	(V-I)	(R-I)	Telescope	Observer
1990 Feb 10.1	7932.6	—	—	> 16.20	—	—	—	—	—	Berkeley Auto SN Search	
1990 Feb 15.1	7937.6	—	—	15.30(20)	—	—	—	—	—	Berkeley Auto SN Search	
1990 Feb 16.1	7938.6	16.18(02)	—	15.35(03)	—	—	—	—	—	CTIO .91m	Baldwin
1990 Feb 17.1	7939.6	16.14(02)	15.70(02)	15.25(03)	—	0.45(03)	0.45(04)	—	—	CTIO .91m	Baldwin
1990 Feb 17.1	7939.6	16.12(03)	15.70(03)	15.24(04)	14.84(04)	0.42(04)	0.46(05)	0.86(05)	0.40(06)	KPNO .91m	Marschall
1990 Feb 18.1	7940.6	16.12(02)	15.68(02)	15.17(03)	—	0.45(03)	0.51(04)	—	—	CTIO .91m	Baldwin
1990 Feb 18.1	7940.6	16.12(04)	15.67(04)	15.23(05)	14.80(05)	0.45(06)	0.44(06)	0.87(06)	0.43(07)	KPNO .91m	Marschall
1990 Feb 21.1	7943.6	—	15.61(04)	15.05(04)	—	—	0.56(06)	—	—	CTIO Schmidt	Weller
1990 Feb 22.1	7944.6	16.08(04)	15.55(03)	15.05(04)	—	0.53(05)	0.50(05)	—	—	CTIO Schmidt	Weller
1990 Feb 24.8	7947.3	16.10(03)	15.60(03)	15.02(04)	14.59(03)	0.51(04)	0.58(05)	1.01(04)	0.42(05)	FLWO 0.61m	Schild
1990 Feb 25.8	7948.3	16.10(03)	15.56(03)	15.03(04)	14.61(04)	0.54(04)	0.53(04)	0.95(05)	0.42(06)	FLWO 0.61m	Schild
1990 Feb 27.8	7950.3	16.11(03)	15.61(02)	15.02(03)	14.58(03)	0.51(04)	0.59(04)	1.03(04)	0.44(04)	FLWO 0.61m	Schild
1990 Feb 28.8	7951.3	16.10(04)	15.59(03)	15.02(04)	14.62(05)	0.52(05)	0.57(05)	0.97(06)	0.40(07)	FLWO 0.61m	Schild
1990 Mar 1.8	7952.3	16.19(03)	15.58(02)	15.00(03)	14.57(03)	0.60(04)	0.58(04)	1.01(04)	0.43(05)	FLWO 0.61m	Schild
1990 Mar 2.8	7953.3	16.18(03)	15.57(02)	14.98(03)	14.57(03)	0.60(04)	0.59(04)	1.00(04)	0.41(05)	FLWO 0.61m	Schild
1990 Mar 3.8	7954.3	16.21(02)	15.55(02)	14.97(03)	14.54(03)	0.64(03)	0.58(04)	1.01(04)	0.43(04)	FLWO 0.61m	Schild
1990 Mar 5.1	7955.6	16.24(01)	—	—	—	—	—	—	—	CTIO .91m	A. Phillips
1990 Mar 7.8	7958.3	—	15.51(02)	14.89(03)	14.44(03)	—	0.62(04)	1.07(04)	0.45(04)	FLWO 0.61m	Schild
1990 Mar 8.8	7959.3	16.32(03)	15.52(02)	14.91(03)	14.45(03)	0.76(04)	0.61(04)	1.07(04)	0.46(04)	FLWO 0.61m	Schild
1990 Mar 9.1	7959.6	16.39(04)	—	—	—	—	—	—	—	CTIO .91m	A. Phillips
1990 Mar 9.8	7960.3	—	—	14.90(06)	—	—	—	—	—	FLWO 0.61m	Schild
1990 Mar 22.8	7973.3	—	15.79(04)	15.01(03)	14.52(04)	—	0.78(05)	1.27(06)	0.49(05)	FLWO 0.61m	Schild
1990 Jun 21.4	8063.9	—	17.47(08)	16.25(03)	15.63(03)	—	1.22(09)	1.84(09)	0.62(04)	CTIO 4m	Navarette
1990 Jun 25.4	8067.9	19.40(16)	17.80(08)	16.51(04)	15.91(04)	1.60(18)	1.29(09)	1.89(09)	0.60(06)	CTIO 4m	Navarette
1990 Jun 29.4	8071.9	19.81(18)	18.27(17)	16.80(08)	16.07(07)	1.54(25)	1.47(19)	2.20(18)	0.73(11)	CTIO 4m	Navarette
1990 Jul 4.4	8076.9	20.41(21)	18.76(08)	17.36(07)	16.64(06)	1.65(22)	1.40(11)	2.12(10)	0.72(09)	CTIO .91m	Suntzeff
1990 Jun 12.4	8084.9	—	18.90(11)	17.44(08)	16.67(07)	—	1.46(14)	2.23(13)	0.77(06)	CTIO .91m	Wells
1990 Aug 1.4	8104.9	20.56(22)	19.01(12)	—	—	1.55(27)	—	—	—	CTIO .91m	Suntzeff
1990 Aug 12.4	8115.9	—	19.30(16)	—	16.99(09)	—	—	2.31(18)	—	CTIO .91m	Wells
1990 Aug 24.4	8127.9	—	19.28(13)	17.90(09)	17.04(09)	—	1.38(16)	2.24(16)	0.86(13)	CTIO .91m	Navarette
1990 Sep 15.3	8149.8	—	19.33(14)	18.20(11)	17.18(09)	—	1.13(18)	2.15(17)	1.02(14)	CTIO .91m	Hernandez
1990 Oct 10.2	8174.7	—	—	18.25(16)	17.51(14)	—	—	—	0.74(21)	CTIO .91m	Suntzeff
1990 Oct 14.2	8178.7	—	—	18.17(10)	17.54(08)	—	—	—	0.63(13)	CTIO 4m	Navarette
1990 Oct 20.3	8184.8	—	19.87(19)	18.39(12)	17.63(09)	—	1.48(22)	2.24(15)	0.76(15)	CTIO .91m	Hernandez
1990 Oct 24.3	8188.8	21.10(30)	19.84(13)	18.56(10)	17.61(08)	1.36(33)	1.28(16)	2.23(15)	0.95(13)	KPNO 2.1m	Porter
1990 Oct 24.3	8188.8	—	19.82(14)	18.58(13)	17.69(08)	—	1.24(19)	2.13(16)	0.89(15)	CTIO .91m	Gonzalez
1990 Nov 9.3	8204.8	—	—	18.72(13)	17.89(12)	—	—	—	0.83(18)	KPNO 2.1m	Saha
1990 Dec 11.2	8236.7	—	20.17(28)	18.73(15)	18.08(13)	—	1.44(32)	2.09(31)	0.65(20)	CTIO 4m	Navarette
1990 Dec 19.2	8244.7	—	20.39(18)	18.94(13)	18.27(12)	—	1.45(22)	2.12(22)	0.67(18)	KPNO 2.1m	Kirshner
1991 Jan 10.1	8266.6	—	—	19.10(16)	—	—	—	—	—	CTIO .91m	Bond
1991 Jan 16.1	8272.6	—	—	19.00(15)	18.37(15)	—	—	—	.63(21)	CTIO .91m	Gonzalez
1991 Sep 9.5	8509.0	—	—	> 20.8	—	—	—	—	—	KPNO 2.1m	Porter

Uncertainties in hundreths of magnitudes are listed in parantheses next to all values.

time ($m_R > 16.2$ mag). Note that this estimate is much brighter than the limit $m_V > 19.0$ mag reported by Pennypacker & Perlmutter (1990). Observations of NGC 1035 were made nearly 600 days (JD=2448509) after the discovery of SN 1990E. In the *R* image, a very faint source is seen at the position of the SN; unfortunately, until another image is obtained, it is impossible to ascertain whether the source is the SN, or simply part of the complex galaxy background. We estimate the brightness of this source by subtracting artificial PSFs of different brightness until the source disappears. The brightness of this object ($m_R = 20.8 \pm 0.3$ mag) provides an upper limit to the brightness of the SN at this epoch.

J and *H* photometric observations were made of SN 1990E for a month following discovery at the FLWO 0.61 m using the SONIC 62×58 pixel Santa Barbara InSb Array. The SN and sky were observed alternately every 30 s. The images are constructed by subtracting the sum of the sky images from the sum of SN images. The resultant image is then corrected with bias, dark, and flatfield images. A standard star at an airmass similar to the SN was observed directly before or after the SN to determine the zero point for the photometry and to calibrate the brightness of Star 1 (Table 1). The pixel scale of the SONIC at the FLWO 0.61 m was very large, 3.5″/pixel, and a majority of the SN's light was concentrated into one pixel, making PSF fitting programs such as DOPHOT pointless. We removed the background by subtracting the galaxy profile (which is quite smooth in the IR) from the image, leaving the SN as a point source. We then measure the relative brightness of the SN and Star 1 with apertures. Our *J* and *H* photometry of SN 1990E is presented in Table 3.

Optical spectra of SN 1990E were obtained at 30 epochs spanning 230 days with instruments on the Hale 5 m, MMT, AAT, Lick 3.1 m, MSSSO 2.3 m, KPNO 2.1 m, CTIO 1.5 m, and FLWO 1.5 m telescopes (Table 4). Spec-

TABLE 3. IR photometry of SN 1990E.

Date (UT)	JD (2440000+)	J	H	Telescope	Observer
1990 Feb 16.1	7938.6	14.56(20)	14.44(20)	FLWO 0.61m	S. Willner
1990 Feb 17.1	7939.6	14.42(20)	14.26(20)	FLWO 0.61m	S. Willner
1990 Feb 21.1	7943.6	14.14(20)	14.21(20)	FLWO 0.61m	S. Willner
1990 Mar 15.1	7965.6	13.57(20)	13.44(20)	FLWO 0.61m	S. Willner

Uncertainties in hundreths of magnitudes are listed in parantheses next to all values.

TABLE 4. Spectrophotometry of SN 1990E.

Date (UT)	JD (2440000+)	Spectral Range (Angstroms)	Telescope	Instrument	Observer
1990 Feb 16.1	7938.6	5100-8900	Palomar 5.0 m	Double Spec	W. Sargent, C. Steidel
1990 Feb 16.1	7938.6	4300-6200	KPNO 2.1 m	Gold Cam	T. Boroson, R. Green
1990 Feb 16.5	7939.0	4600-9800	AAT 3.9 m	CCD Spec	R. Stathakis, R. Cannon
1990 Feb 17.1	7939.6	4700-6600	KPNO 2.1 m	Gold Cam	T. Boroson, R. Green
1990 Feb 17.1	7939.6	4500-7000	FLWO 1.5 m	Reticon	J. Peters
1990 Feb 18.1	7940.6	4700-6600	KPNO 2.1 m	Gold Cam	T. Boroson, R. Green
1990 Feb 18.1	7940.6	4500-7000	FLWO 1.5 m	Reticon	J. Peters
1990 Feb 19.1	7941.6	5400-7300	KPNO 2.1 m	Gold Cam	T. Boroson, R. Green
1990 Feb 19.4	7941.9	3200-5700	MSSSO 2.3 m	PCS	K. Freeman
1990 Feb 20.1	7942.6	4000-7200	Lick 3.1 m	UV Schmidt	D. Womble
1990 Feb 20.1	7942.6	4700-6600	KPNO 2.1 m	Gold Cam	T. Boroson, R. Green
1990 Feb 20.1	7942.6	4500-7000	FLWO 1.5 m	Reticon	E. Horine
1990 Feb 21.1	7943.6	4500-7000	FLWO 1.5 m	Reticon	E. Horine
1990 Feb 22.1	7944.6	4200-8900	Lick 1.0 m	CCD Spec	R. Stone
1990 Feb 23.0	7945.5	3200-8000	CTIO 1.5 m	CCD Spec	L. Wells
1990 Feb 23.1	7945.6	6200-7200	KPNO 2.1 m	Gold Cam	J. Halpern
1990 Feb 23.1	7945.6	4500-7000	FLWO 1.5 m	Reticon	J. Peters
1990 Feb 24.1	7946.6	4500-7000	FLWO 1.5 m	Reticon	J. Peters
1990 Feb 25.1	7947.6	4500-7000	FLWO 1.5 m	Reticon	A. Zabludoff
1990 Feb 27.1	7949.6	4500-7000	FLWO 1.5 m	Reticon	A. Zabludoff
1990 Feb 28.2	7950.7	4500-7000	FLWO 1.5 m	Reticon	A. Zabludoff
1990 Mar 2.1	7952.6	4500-7000	FLWO 1.5 m	Reticon	E. Horine
1990 Mar 3.1	7953.6	4500-7000	FLWO 1.5 m	Reticon	E. Horine
1990 Mar 4.0	7954.5	3200-9000	CTIO 1.5 m	CCD Spec	M. Phillips
1990 Mar 7.1	7957.6	5900-8900	Lick 1.0 m	CCD Spec	R. Stone
1990 Mar 19.1	7969.6	4400-8800	MMT	Red Channel	R.C. Smith, R. Kirshner
1990 Jul 3.4	8075.9	3800-7800	CTIO 1.5 m	CCD Spec	M. Phillips
1990 Jul 31.3	8103.8	3900-7100	Lick 3.1 m	CCD Spec	A. Filippenko, J. Shields
1990 Oct 20.3	8184.8	5900-8900	Lick 3.1 m	CCD Spec	A. Filippenko, J. Shields
1990 Nov 12.3	8207.8	3800-8800	MMT	Red Channel	R.C. Smith, J. Raymond

trographs on all telescopes except the FLWO 1.5 m were used in long slit mode, which allows the galaxy and sky background to be fit and subtracted from the spectrum of the supernova, at least to first order. Spectra from the FLWO 1.5 m telescope were obtained using a two-beam photon counting spectrograph. Background subtraction with this instrument is accomplished by placing one aperture on a region of the galaxy near the supernova, while the other aperture is integrating on the object. Although this process does not remove the background as accurately as using a long slit, it does an adequate job while the supernova is bright. Standard stars were observed for flux calibration and removal of instrumental sensitivity variations. At later times, even long slit spectral observations were extremely difficult due to the brightness of the galaxy at the position of the supernova, and accurate background subtraction in these spectra is nearly impossible. We have calibrated the flux scale of these spectra using the R photometry. The R magnitude for the spectra is synthesized using analytic filter functions (Bessell 1990) and matched to the R photometry by multiplying the spectra by a constant. Additional spectroscopic observations have been reported in the IAU circulars (Benetti *et al.* 1990; Lopez *et al.* 1990; Lopez 1990; Lopez & Gomez 1991).

3. RESULTS AND DISCUSSION

The optical and near-infrared photometric evolution of SN 1990E is displayed in Fig. 3. These observations indicate that the supernova reached B maximum ($m_B^{\max} = 16.08 \pm 0.03$ mag on JD=2447944±1) a week after discovery, and that the V ($m_V^{\max} = 15.50 \pm 0.04$ mag on JD=2447960±5), R ($m_R^{\max} = 14.89 \pm 0.04$ mag on JD =2447960±5), and I ($m_I^{\max} = 14.44 \pm 0.04$ mag on JD =2447960±5) maxima occurred approximately two weeks later. The B maximum is distinct and narrow, whereas the V, R, and I maxima are very broad.

Although the IR photometric coverage of the SN is poor, it is apparent that SN 1990E increased in brightness by nearly a magnitude in the J and H bands during the month following discovery. SN 1990E is the first SN II-P (other than SN 1987A) to have a published J and H light curve, but its IR photometric behavior is not unexpected. After explosion, SNe II-P cool slowly to the recombination temperature of hydrogen, radiating energy deposited into the hydrogen from the initial shock. This produces the plateau in the light curve during which the expansion and cooling of the photosphere usually balance each other so that the optical luminosity remains more or less constant. The near-IR, on the other hand, is in the Rayleigh–Jeans regime where the flux depends only linearly on the temperature. In these bandpasses the increased flux due to expansion of the photosphere is more significant than the decreased flux resulting from cooling, and consequently the near-IR luminosity of the SN increases with time. In cases where the velocity of a SN's photosphere evolves slowly, the surface area of the photosphere could increase at a sufficient rate so that the IR light curve would continue to rise until the SN becomes optically thin and falls off the plateau. In other SNe, where the velocity of the photosphere evolves quickly through the entire plateau phase, the light curve could easily resemble that of the SN II-L class—especially in the U and B bands. A good example of this behavior is exhibited by the two SNe II-L, SN 1980K and SN 1979C. These SNe exhibit a nearly linear decline in their U and B light curves from maximum to the radioac-

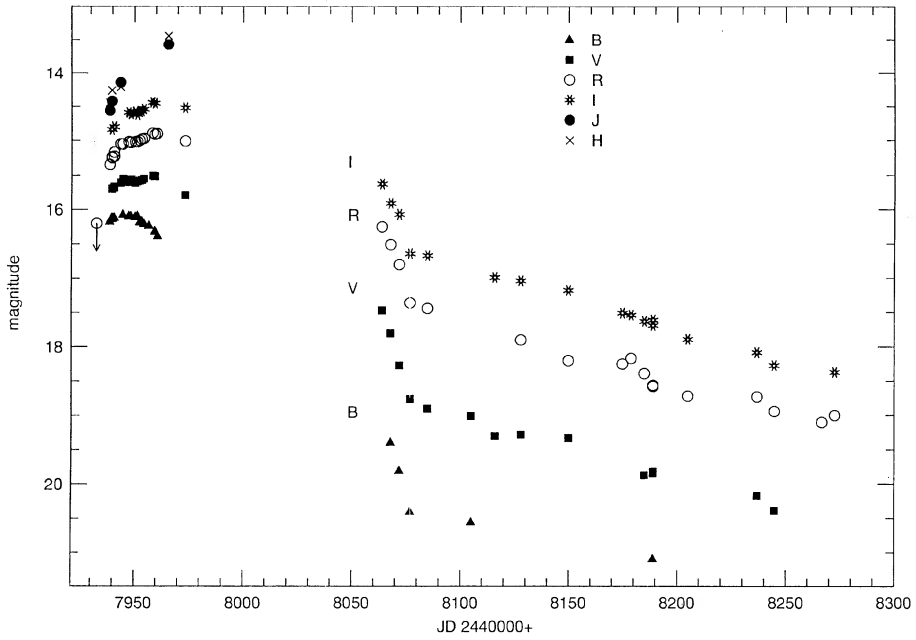

FIG. 3. *BVRIJH* photometry of SN 1990E.

tive tail. In *V*, however, their light curves resemble that of SNe II-P: the initial decline of the light curve is slower than in *U* and *B*, and the light curve falls sharply to the radioactive tail (de Vaucouleurs *et al.* 1981; Barbon *et al.* 1982a; Barbon *et al.* 1982b). Furthermore, observations made by Dwek *et al.* (1983) show SN 1980K declined much more slowly in the near IR (*JHKLL'*), and presumably even more closely followed the light curve of a SN II-P at these wavelengths.

Four weeks after *B* maximum SN 1990E became lost into the evening twilight. It appears that the SN may have gradually declined in brightness in *B, V, R,* and *I* until photometric observations of SN 1990E were resumed 90 days later. At this time SN 1990E was still quite bright, but fading rapidly. After falling in brightness by nearly 1.5 mag in *V* in just 13 days, SN 1990E abruptly slowed its rate of decline to approximately 0.90 mag/100^{d} in the optical, and continued to fade at this rate for at least another 200 days. This behavior, as we will show later, is similar to SN 1969L, and is typical for SNe II-P.

The $(B-V)$, $(V-R)$, $(V-I)$ color evolution of SN 1990E is plotted in Fig. 4. The earliest observations of SN 1990E show that it was not a particularly blue object with $(B-V)=0.45\pm0.03$ mag, $(V-R)=0.45\pm0.04$ mag, and $(V-I)=0.88\pm0.04$ mag. The color of SN 1990E during the month following discovery evolved quickly to the red. After being recovered in June, the color continued to evolve to the red as it fell from the plateau and then remained essentially constant in color throughout the remainder of our observations. During the photospheric phase, the continua of SNe II-P resemble Planck functions (Kirshner & Kwan 1974) at a temperature which can be measured from the observed colors of the SNe. Figure 5 displays the color temperature evolution of SN 1990E, computed using the *BVI* photometry and assuming $A_V=1.5$ mag (derived below). We exclude the *R* band because of contamination from Hα. The color temperature was determined by performing a chi-squared minimization between the photometry and the synthesized colors of

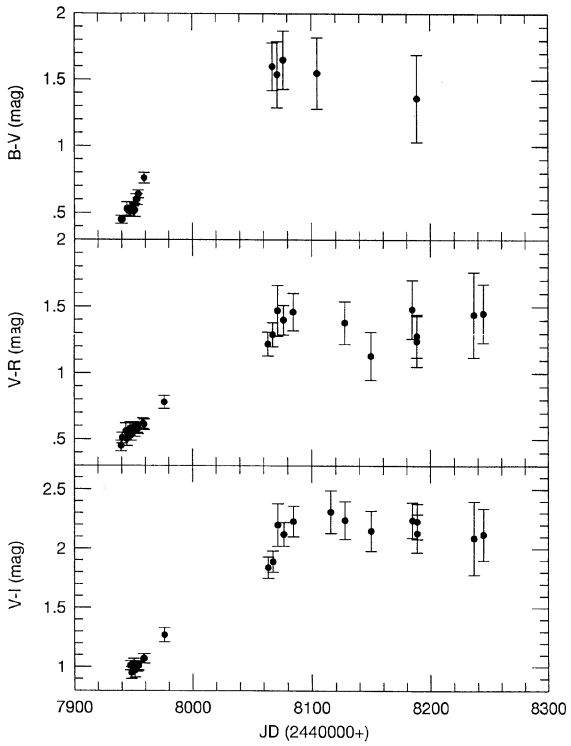

FIG. 4. $(B-V)$, $(V-R)$, and $(V-I)$ color curves for SN 1990E.

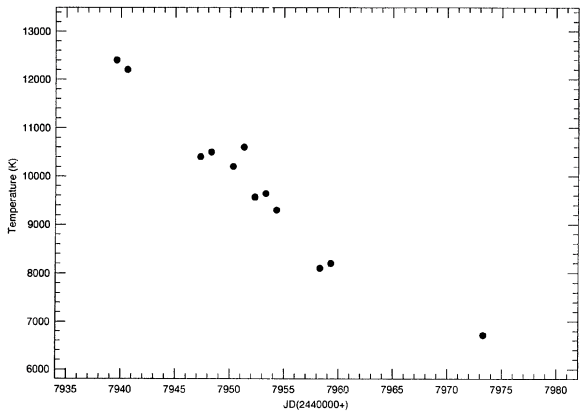

FIG. 5. The color temperature evolution of SN 1990E presented as a function of time. The color temperature was measured by performing a chi-squared minimization between the observed *BVI* photometry and photometry synthesized from a blackbody. The photometry was dereddened using the extinction law of Whitford (1958) and a value of $A_V=1.50$ mag.

Planck functions. The photometry was synthesized using the analytic filter functions of Bessell (1990) with zero points derived from spectrophotometry of Vega (Hayes *et al.* 1975) and the photometry of Johnson & Morgan (1953). Near the time of discovery, SN 1990E was very hot ($\approx$13000 K), but it cooled down to 6500 K within a month (Fig. 5). This evolution is comparable to other SNe II-P but is much slower than SN 1987A which cooled over a comparable temperature range in approximately two weeks (Menzies *et al.* 1987). The color temperatures are used in the next section to determine the bolometric light curve (the values are listed in Table 6). We expect our method of measuring the color temperature to be reliable for most SNe until several weeks after the explosion. At this point most SNe have cooled to below $T<6000$ K, and line blanketing cuts out a significant fraction of the continuum flux in the *B* band.

Our spectra are displayed in Fig. 6, and the line identifications and their observed wavelengths are listed in Table 5. The coverage of SN 1990E at early times is especially good. The spectra exhibit most of the lines seen in SN 1969L (Ciatti *et al.* 1971; Kirshner & Kwan 1974) and SN 1987A (Phillips *et al.* 1988). The earliest spectra, taken within 24 hours of discovery, show a broad P-Cygni profile of Hα with the fastest material blueshifted to 15 000 km s^{-1}. The P-Cygni profiles of lines of He I λ5876 and Hβ also exhibit similar velocity widths. In addition, there are weak lines at $\lambda_{\rm lab}\approx$5700 Å, $\lambda_{\rm lab}\approx$5500 Å, and $\lambda_{\rm lab}\approx$4600 Å (we have corrected for the expansion of the SN photosphere using He I 5876 as a guide). These lines, which persist for only the first few days following discovery, we identify as N II transitions centered at λ5679 ($3s^3P^0$–$3p^3D$), λ5537 ($3p^3P$–$3d^3P^0$), and λ4623 ($3s^3P^0$–$3p^3P$), respectively. These are strong lines which lie approximately 18 eV above the ground state and are observed in B-type stars (Merrill 1958). SN 1990E appears to have had the high temperature (Figs. 5 and 7) needed to excite

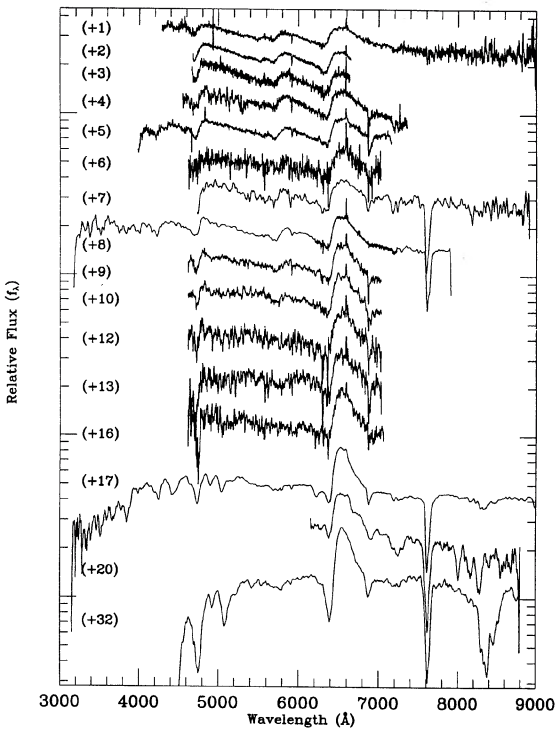

FIG. 6. The photospheric phase spectral observations of SN 1990E. The age is given in days after the date of discovery, JD=2447938. Observations from the same days have been combined. The spectra have not been corrected for the redshift of the galaxy, 1270 km s^{-1}. The first spectrum (+1) has been corrected for atmospheric absorption in the *A* band ($\approx$7000 Å) and *B* band ($\approx$6860 Å).

N II to this level during the time when these lines were observed. The other set of strong optical N II transitions, centered at λ5010 ($3p^3D$–$3d^3F^0$), were not seen in the spectra because they coincide with the emission of Hβ, which fills in these lines and obscures them.

He I λ5876 increased in strength for the first 3 days following discovery and then gradually faded away so that 10 days later it was no longer seen. Fe II λ5169 and λ5018 appeared 10 and 15 days (respectively) after discovery and increased in strength as the SN evolved. A strong feature in SN 1987A, attributed to a blend of the Ba II λ4554 resonance line and several Fe II lines (Williams 1987), was also seen in SN 1990E approximately 15 days after discovery, as well as the infrared Ca II triplet $\lambda\lambda$8498, 8542, 8662 and a line observed at λ6230 Å, which we attribute to Si II λ6355. This line of Si II has also been identified by Filippenko & Sargent (1986) and Filippenko (1992) as being visible in SN 1985L. Branch (1987) has suggested, on the basis of LTE calculations of line strengths, that this resonance line of silicon would likely be visible in SNe II spectra and should be most prominent while a SN is at a temperature between 8000–10000 K—the temperature range of SN 1990E while this line was observed (Figs. 5 and 7). In the final spectrum obtained of SN 1990E before it disappeared behind the Sun (32 days after discovery), the Ca II infrared triplet had become very strong, and lines of Sc II λ5526 and λ5658 were beginning to appear.

TABLE 5. Line identifications and observed wavelengths of absorption features early time spectrophotometry of SN 1990E.

JD (2440000+)		7939	7940	7941	7942	7943	7944	7945	7946	7947	7948	7950	7951	7954	7955	7958	7970
identification	λ_{rest} (Å)	Observed Wavelength (Å)															
Ca II	3945	—	—	—	—	—	—	—	—	—	—	—	—	—	3848	—	—
Hγ	4201	—	—	—	—	4210	—	—	4223	—	—	—	—	—	4242	—	—
N II	4623	4461	—	—	—	—	—	—	—	—	—	—	—	—	—	—	—
Ba II+FeII	4554	—	—	—	—	—	—	—	—	—	—	—	—	—	4426	—	—
Hβ	4861	4701	4692	4699	4692	4708	4706	4711	4703	4721	4731	4725	4715	4739	4744	—	4752
Fe II	5018	—	—	—	—	—	—	—	—	—	—	—	—	—	4916	—	4928
Fe II	5169	—	—	—	—	—	—	—	5010	—	—	—	—	5047	5047	—	5083
N II	5537	5314	—	—	—	—	—	—	—	—	—	—	—	—	—	—	—
Sc II	5526	—	—	—	—	—	—	—	—	—	—	—	—	—	—	—	5423
N II	5679	5487	5518	5527	5522	5555	—	—	—	—	—	—	—	—	—	—	—
Sc II	5658	—	—	—	—	—	—	—	—	—	—	—	—	—	—	—	5539
He I	5876	5682	5675	5693	5693	5701	5726	5697	5707	5714	5711	—	—	—	5734	—	—
Na I	5889+5995	—	—	—	—	—	—	—	—	—	—	—	—	—	—	—	5781
Si II	6355	—	—	—	—	—	—	—	—	—	—	—	—	6222	6228	—	—
Hα	6563	6302	6315	6320	6338	6347	6345	6342	6355	6360	6351	6358	6372	6363	6379	6379	6390
Ca II	8498+8542+8662	—	—	—	—	—	—	—	—	—	—	—	—	—	8332	—	8376

Hydrogen lines were seen throughout the evolution of SN 1990E. At the earliest times, lines as far down the Balmer series as Hζ (3889 Å) were visible, as extremely broad weak lines. As SN 1990E evolved, the Hα P-Cygni profile gradually became narrower and gained prominence, while the other Balmer lines become obscured by metal lines. This gradual evolution is in marked contrast to SN 1987A, where Hα became very strong within a few days of discovery. In addition, narrow Na D lines λλ5890, 5896 were visible as a marginally resolved doublet with a total equivalent width of 1.6±0.1 Å at the recession velocity of NGC 1035 (1270 km s^{-1} as measured from our spectra). These lines did not evolve in time, and we attribute them to the interstellar medium of NGC 1035.

In the spectra of SN 1990E, SN 1969L (Ciatti *et al.* 1971; Kirshner *et al.* 1974), and SN 1987A (Menzies *et al.* 1987; Blanco *et al.* 1987), He I λ5876 was prominent at early times while these SNe were very hot. Fe II λ5169 and λ5018 appeared at about the time that He I λ5876 disappeared, and other lines such as Sc II λ5526 and λ5658 became visible when the SNe had cooled substantially. The appearance and disappearance of these absorption lines in SNe II-P should depend primarily on the temperature of the photosphere. The absorption lines, therefore, give information about the temperature of SNe at different stages of their evolution.

The extinction of SN 1990E can be estimated in several ways. We expect the He I λ5876 line to disappear when the SN has cooled to a specific temperature. With this fact in mind, we compare the *BVI* colors of SN 1990E to SN

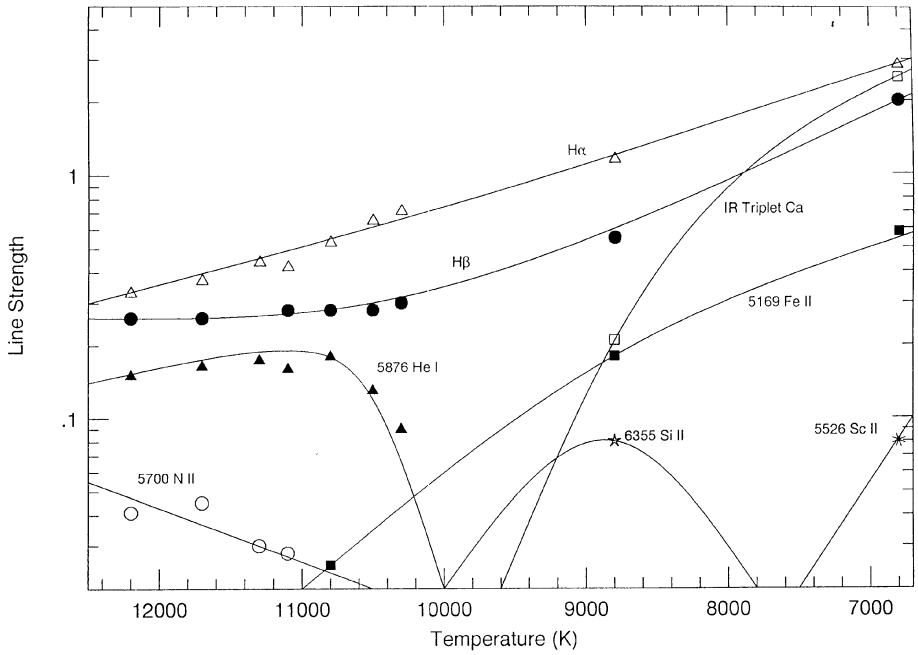

FIG. 7. The strength of several lines is plotted as a function of the *BVI* color temperature for SN 1990E. Approximate fits to the observations are shown to clarify the diagram. Strength is defined as $(f_\lambda^{max}-f_\lambda^{min})/f_\lambda^{min}$, where f_λ^{max} and f_λ^{min} are the flux of the maximum and minimum of a line profile.

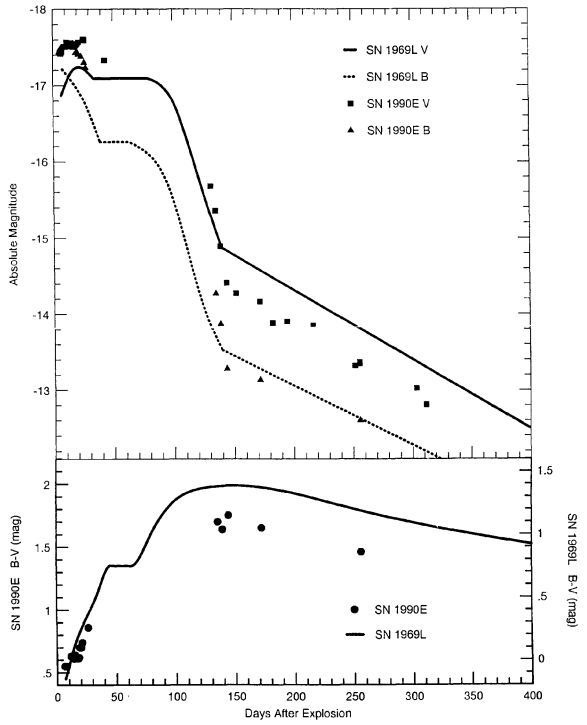

FIG. 8. Comparison of the absolute magnitude and $(B-V)$ light curves of SN 1990E and SN 1969L (Ciatti *et al.* 1971). Distances of 21 and 11 Mpc are assumed for the two SNe, respectively. The extinction in B and V is taken to be $A_V=1.50$ mag and $A_B=2.00$ mag for SN 1990E, and $A_V=0.18$ mag and $A_B=0.24$ mag for SN 1969L. The $(B-V)$ scales are offset by 0.45 mag to reflect the color excess of SN 1990E with respect to SN 1969L at early times.

1987A (Hamuy *et al.* 1988) on the first day after the He I λ5876 was no longer visible, JD=2447956 and JD =2446854 (Phillips *et al.* 1988), respectively, for the two SNe. Using the reddening law of Whitford (1958), the color difference between the two SNe is minimized to determine the extinction. Assuming the extinction to SN 1987A is $A_V=0.45\pm0.15$ mag (see discussion in Arnett *et al.* 1989), we derive a visual extinction to SN 1990E of $A_V=1.5\pm0.3$ mag.

Another method of estimating the extinction to SN 1990E is to assume that its $(B-V)$ evolution is the same as that of SN 1969L. The color evolution of these two SNe is shown in Fig. 8, and we find that SN 1990E has a $(B-V)$ excess of approximately 0.45 ± 0.1 mag at early times and 0.15 ± 0.1 mag at late times compared to SN 1969L. Because of the large uncertainties in the B photometry due to the faintness of the SNe and systematic errors caused by an emission-line object being observed with detectors (CCDs and photographic plates) that have significantly different effective bandpasses, we believe that the comparison at early times gives a much more accurate estimate of SN 1990E's reddening. SN 1969L is thought to have only a small amount of reddening due to our Galaxy, $E(B-V)=0.06$ mag (Burstein & Heiles 1984), and to its host galaxy NGC 1058, $E(B-V)=0.0$ mag (Kirshner & Kwan 1974), and we can use the relation $A_V=3E(B-V)$ (Whitford 1958) to estimate the total extinction to SN 1990E to be $A_V=1.53\pm0.3$ mag. These methods of determining the reddening show satisfactory agreement, and we adopt a value of $A_V=1.5\pm0.3$ mag for the visual extinction to SN 1990E. Burstein & Heiles (1984) estimate that our Galaxy dims NGC 1035 by only $A_V=0.02$ mag; therefore the extinction that SN 1990E suffers is from dust in its host galaxy.

The observed recession velocity of NGC 1035, 1237 km s^{-1} (Sandage & Tammann 1981), corrected for Galactic rotation and Virgo infall, yields a true velocity of recession of $v_{\rm rec}=1150$ km s^{-1} (Schmidt *et al.* 1992). The correction for Virgo infall is small and the exact parameters of the infall model are not important. The distance derived to NGC 1035 from the Hubble law is then $23>D>13$ Mpc for $50<H_0<90$ km s^{-1} Mpc^{-1}. Schmidt *et al.* (1992) have estimated the distance to SN 1990E to be 21 ± 3 Mpc using the Expanding Photosphere Method on a subset of the data presented here. In addition, the data of Aaronson *et al.* (1986), used in conjunction with the IR Line Width–Velocity calibration of Freedman (1990), gives a distance to NGC 1035 of 15.9 Mpc. Assuming that SN 1990E suffers from a visual extinction of $A_V=1.50\pm0.30$ mag as derived above, the absolute magnitude of the supernova is $M_V^{\rm max}=(-17.61\pm0.3)-5\log(D/21\ {\rm Mpc})$ mag. The B and V light curves of SN 1990E are compared to SN 1969L in Fig. 8. Absolute magnitudes are plotted, assuming the extinction discussed above and distances of 21 and 11 Mpc (Schmidt *et al.* 1992), respectively, for the two SNe. The shapes of the two light curves are similar, and the plateau phases of the two SNe appear to be almost identical in length. The fall off the plateau to the exponential tail, though poorly sampled, is larger and more precipitous in the case of SN 1990E. This suggests that relative to SN 1969L, SN 1990E either ejected less ^{56}Ni or had more energy deposited into its envelope by the shock. The exponential tails of the two light curves fall off at similar rates (e-folding time $\approx$120 days) and are in accord with the light curves being powered by the radioactive decay of ^{56}Co (111.3 days) during this phase of evolution.

The end of the photometric plateau also signals the onset of the nebular spectrum in SNe II-P. The nebular phase spectra for SN 1990E are displayed in Fig. 9. After SN 1990E reappeared in the morning sky, our first spectrum was obtained just after SN 1990E finished its fall from the plateau. This observation, taken on JD=2448076 (138 days after discovery), shows the SN making the transition to the nebular phase. Relatively broad P-Cygni profiles of Hα and Na I $\lambda\lambda$5890, 5896 were still seen, and nebular emission of [O I] $\lambda\lambda$6300, 6363 emerged along with a feature which is probably a blend of [O II] $\lambda\lambda$7320, 7330 and [Ca II] $\lambda\lambda$7292, 7324. In addition, Fe II λ5169 was still seen in absorption at a velocity of 4000 km s^{-1}. Four weeks later (166 days after discovery), although Hα had narrowed considerably, the supernova's spectrum had shown little evolution. By the middle of October (247 days after discovery) Hα showed broad (FWHM$\approx$3000 km s^{-1}) and narrow (FWHM$<$1100 km s^{-1}) components. In addition, a broad emission feature, which we at-

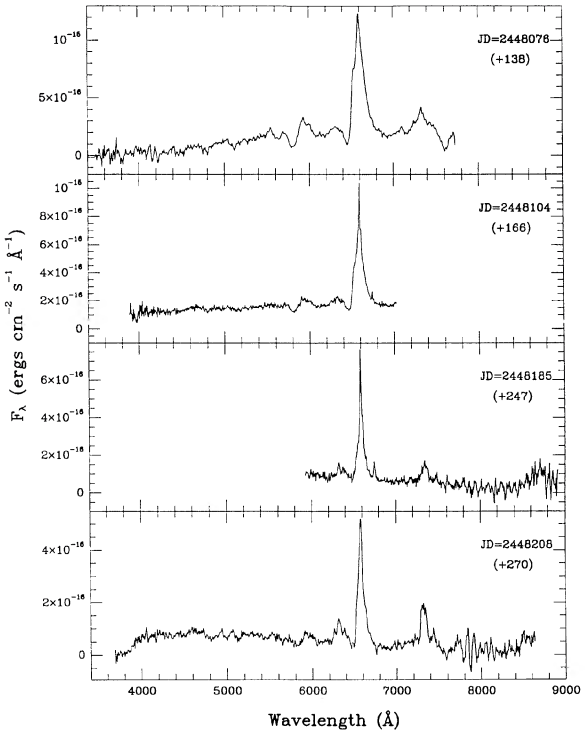

FIG. 9. Spectral observations of SN 1990E in the nebular phase.

tribute to the IR calcium triplet ($\lambda\lambda$8498,8542,8662) appeared at $\approx$8600 Å (outside the spectral range of previous observations). Our final spectral observation of SN 1990E, taken approximately 9 months after discovery, shows the [O II]+[Ca II] feature at 7300 Å and the [O I] feature at 6300 Å having gained in strength relative to Hα.

The flux in Hα and [O I] $\lambda\lambda$6300, 6363 for SN 1990E as a function of time is displayed in Fig. 10. The energy emitted by the supernova in Hα decayed exponentially in time roughly at the ^{56}Co rate. However, the flux in [O I] appears

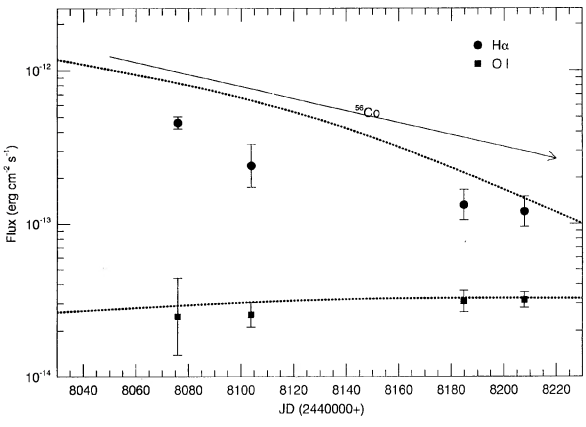

FIG. 10. The flux in Hα and [O I] $\lambda\lambda$6300, 6363 as a function time for SN 1990E corrected for A_V=1.50 mag. The arrow gives the ^{56}Co decay rate, and the dotted lines refer to the predicted flux of Hα and [O I] $\lambda\lambda$6300, 6363 from model "C" of Chugai (1988).

to be constant as the SN evolves. This result is in contrast to SN 1980K, a SN II-L, for which both Hα and [O I] $\lambda\lambda$6300, 6363 declined at the ^{56}Co rate (Uomoto & Kirshner 1986) for the first 600 days, but is similar to the behavior observed for SN 1986J 4 to 7 years after maximum (Leibundgut *et al.* 1991) and SN 1970G (Kirshner *et al.* 1973; Chugai 1982). For SN 1986J, however, the Hα and [O I] lines exhibit substantially different widths, which indicates that the two lines are probably formed in different regions; this is not apparent for SN 1990E. Chugai (1988) has modeled the Hα and [O I] light curves for SNe II assuming that the material is energized by the decay of ^{56}Co to ^{56}Fe. These models reproduce the observations of SN 1970G and qualitatively match our observations of SN 1990E (Fig. 10). However, the Hα emission decayed at the ^{56}Co rate for a longer period of time in the case of SN 1990E, and this suggests, from Chugai's models, that this SN had a more massive hydrogen envelope than SN 1970G.

Leibundgut *et al.* (1991) have calculated the line ratios for oxygen as a function of the temperature and density of the emitting region for several transitions: 6300:6363, 8446:(6300+6363), and 5577:(6300+6363). From the spectra taken on JD 2448185 and 2448208, we measure (or place limits) on the line ratios for SN 1990E at this time of (6300:6363)=0.65±0.1. 8446:(6300+6363)<0.3, and 5577:(6300+6363)<0.4. Taking the age of the SN to be 270 days and using Figs. 6, 7, and 8 of Leibundgut *et al.*, we derive the temperature, $4000 < T < 6000$ K, and density, $2 \times 10^9 < n_{\rm O\,I} < 5.4 \times 10^9$ cm^{-3} of the oxygen emitting region. Uomoto (1986) has shown that if the [O I] is above its critical density (which is much less than 10^9 cm^{-3}) and has zero optical depth (see discussion in Leibundgut *et al.* 1991), the oxygen mass is given by

$$\mathcal{M}(\mathrm{O\,I}) > 10^8 F(\mathrm{O\,I})\, D^2 e^{2.28/T_4} \mathcal{M}_\odot , \qquad (1)$$

where F(O I) is the observed flux in [O I] $\lambda\lambda$6300, 6363 in ergs cm^{-2} s^{-1}, D is the distance to the object in Mpc, and T_4 is the temperature in units of 10^4 K. Equation (1) and the observed flux in O I ($F_{\rm O\,I} = 3 \times 10^{-14}$ ergs cm^{-2} s^{-1}), yield $\mathcal{M}_{\rm O\,I} > 0.39\mathcal{M}_\odot (D/21\ \mathrm{Mpc})^2$ for T=4800 K and $\mathcal{M}_{\rm O\,I} > 0.05\mathcal{M}_\odot (D/21\ \mathrm{Mpc})^2$ for T=6000 K. This mass range is similar to that found for SN 1980K (Uomoto 1986) and SN 1986J (Leibundgut *et al.* 1991).

Eastman & Kirshner (1989) and Schmutz *et al.* (1990) have demonstrated that the velocity of the material at the photosphere of SNe II can be derived from optically thin lines such as those formed in the optical region by Fe II and Sc II. Figure 11 shows the expansion velocity of the supernova derived from Fe II λ5169 absorption corrected for the observed recession velocity of NGC 1035. Eight days after discovery, when the Fe II lines were first visible, the supernova photosphere was formed in material expanding at $\approx$10 400 km s^{-1}, and 24 days later (32 days after discovery), the photosphere was formed in material traveling at 6500 km s^{-1}. This evolution is substantially slower than SN 1987A (Phillips *et al.* 1988), but is similar to other SNe II-P such as SN 1969L (Ciatti *et al.* 1971; Kirshner & Kwan 1974). Models for supernovae arising from red su-

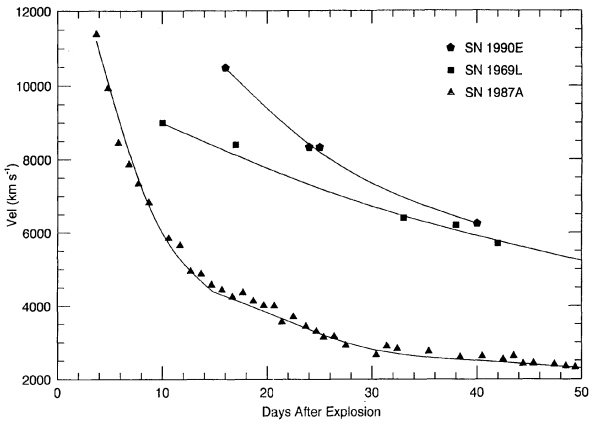

FIG. 11. The velocity of material at the position of the photosphere as a function of time, determined from the absorption of Fe II λ5018 and λ5169 for SN 1990E, SN 1987A, and SN 1969L. The times of explosion are taken from Schmidt *et al.* (1992).

pergiants predict a slower velocity evolution as well as a more rapid rise to maximum luminosity compared to less extended stars (Woosley & Weaver 1986). We conclude that the progenitor of SN 1990E was extended compared to a B3 (blue) supergiant, SN 1987A's progenitor (Arnett *et al.* 1989), and was most likely a red supergiant at the time of explosion.

4. BOLOMETRIC LIGHT CURVE

A bolometric light curve is extremely useful for constraining models of SNe explosions. Attempts at producing these light curves have been made for the SNe Ib/c 1984L and 1987M by Schlegel & Kirshner (1989) and by Nomoto *et al.* (1990), respectively. Unfortunately, measuring the bolometric flux from a supernova with only optical photometry or spectrophotometry is difficult; at early times most of the energy is emitted blueward of 4000 Å, and at late times redward of 1 μ (Suntzeff & Bouchet 1990). These problems can be circumvented in part for SNe II; during the photospheric phase, the continua of SNe II are nearly Planckian (Kirshner & Kwan 1974), and the bolometric luminosity can be approximated by

$$L_{\rm bol}=\frac{4\sigma T_{\rm opt}^4 D^2 f_\lambda}{B_\lambda(T_{\rm opt})}, \qquad (2)$$

where D is the distance to the SN, $T_{\rm opt}$ is the color temperature of the supernova, f_λ is the observed flux density of the supernova, and $B_\lambda(T_{\rm opt})$ is the Planck function evaluated at $T_{\rm opt}$ (discussed in Sec. 3). Models of SN 1990E that include the effects of spherical geometry, treat all important relativistic effects to an accuracy of v/c, and employ non-LTE equations of statistical equilibrium for H and He I show that for the first several weeks, this primitive method gives the correct value for the bolometric luminosity to about 15% (Eastman *et al.* 1993).

As a supernova falls from the plateau and enters the nebular phase, its spectrum loses its Planckian form, and we are forced to simply sum the flux in the bandpasses. At this point SN 1990E had faded sufficiently so that it was no longer detectable above the underlying starlight in B, further complicating matters. SN 1987A was observed over a wide spectral range and is the only SN II for which an accurate bolometric light curve has been constructed (Suntzeff & Bouchet 1990). It is possible to derive corrections for the flux of SN 1990E at wavelengths we were unable to observe by using the observations of SN 1987A. For SN 1987A, the fraction of the energy leaving the supernova in the V, R, and I bands is shown in Fig. 12. This fraction is measured by comparing the flux in VRI (Hamuy *et al.* 1988) to the bolometric flux measured by Suntzeff & Bouchet (1990). After the plateau phase, $L_{VRI}/L_{\rm Bol} \approx 0.4$ for SN 1987A (corrected for extinction), and it does not change much; we take this value as the bolometric correction for SN 1990E. These corrections should be valid because we expect SN II to behave similarly in the nebular phase for many months. During this time the SN shell has expanded long enough so that the differences in the progenitors are no longer important but not so long that the interstellar medium is important. Figure 13 compares the spectra of SN 1987A (Phillips *et al.* 1988) and SN 1980K (Uomoto & Kirshner 1986) to SN 1990E 9 months after discovery; the similarity of these three SNe II, which were very different at maximum, shows that they have similar energy distributions where we can observe them. Dust formation could be a problem. In the cases of SN 1980K and SN 1987A, the only two SNe where dust formation has

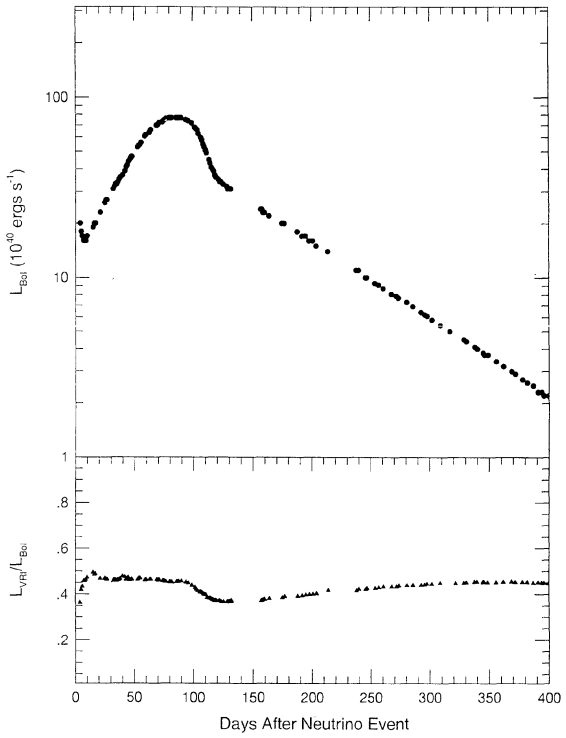

FIG. 12. The bolometric light curve of SN 1987A as determined by Suntzeff & Bouchet (1990), and the fraction of the luminosity of SN 1987A emerging in wavelengths covered by V, R, and I broadband filters.

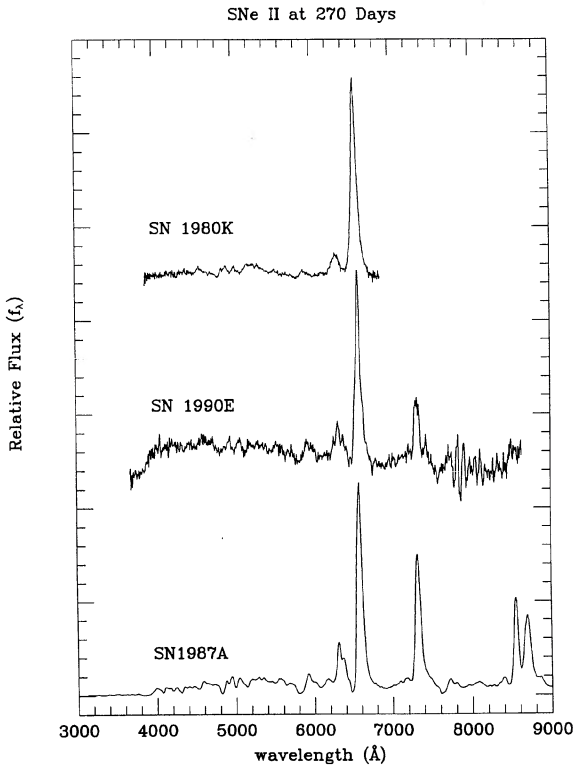

FIG. 13. The spectra of SN 1980K (Uomoto & Kirshner 1986), SN 1990E, and N 1987A (Phillips *et al.* 1988) approximately 270 days after discovery.

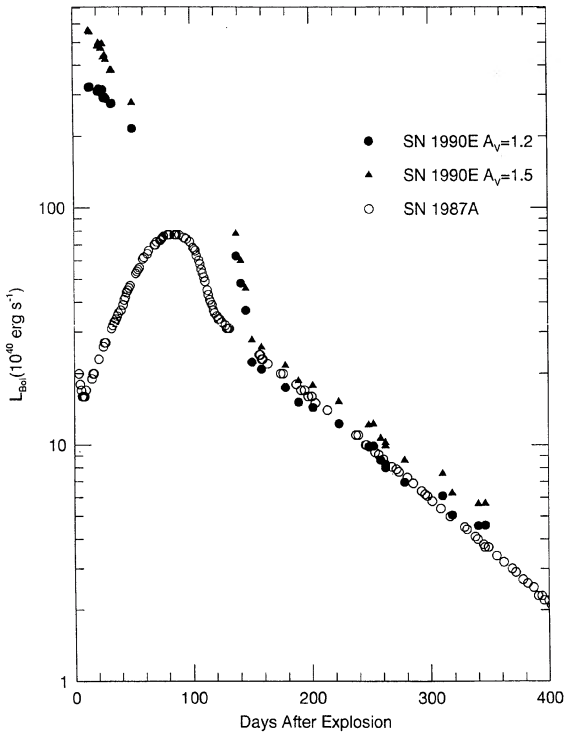

FIG. 14. The bolometric light curve of SN 1990E compared to SN 1987A (Suntzeff & Bouchet 1990). For 1990E, a distance of 21 Mpc is assumed. Calculations using two values for the visual extinction (A_V=1.2 mag and A_V=1.5 mag) are displayed to show the effect of reddening on the light curve.

been observed (Dwek 1983, 1990), the formation of dust suddenly reddened the *BVRI* light curve, but was not observed for SN 1990E. Furthermore, the formation of dust for these two SNe took place more than 500 days after the explosion, while we are considering times when SN 1990E is less than 340 days old.

Figure 14 compares the bolometric light curve of SN 1990E (Table 6) to that of SN 1987A (Suntzeff & Bouchet 1990) assuming a distance of 21 Mpc for NGC 1035 and two values for the extinction to SN 1990E, A_V=1.2 mag and A_V=1.5 mag. Although the value taken for extinction affects the shape of the bolometric light curve at early times, it appears that regardless of the choice of A_V, the bolometric light curve of SN 1990E was not rising at discovery. Yet SN 1990E appears to have been found quite soon after its explosion; at the time of discovery SN 1990E was brightening rapidly in the optical, and its spectra reveal features that evolve on the time scale of a few days. A more quantitative approach is to apply the Expanding Photosphere Method to the data. Schmidt *et al.* (1992) discuss this method in detail and find an explosion date for SN 1990 of JD=2447932 (5 days before discovery). We conclude that this SN (and presumably other SNe II-P) has an extremely sharp rise to bolometric maximum. This result is not unexpected: bolometric light curves have been calculated for SNe II resulting from extended progenitors by Woosley & Weaver (1986), and these models predict

TABLE 6. The bolometric light curve of SN 1990E.

Date (UT)	Julian Date (244000+)	T^a_{BVI} (K)	$\log_{10}(L)^{a,b}$ (ergs s^{-1})	T^c_{BVI} (K)	$\log_{10}(L)^{b,c}$ (ergs s^{-1})
1990 Feb 17.1	7939.6	12400	42.748	10200	42.509
1990 Feb 18.1	7940.6	12200	42.744	10000	42.511
1990 Feb 24.8	7947.3	10400	42.683	8800	42.491
1990 Feb 25.8	7948.3	10500	42.697	8900	42.501
1990 Feb 27.8	7950.3	10200	42.674	8700	42.487
1990 Feb 28.8	7951.3	10600	42.694	9000	42.498
1990 Mar 1.8	7952.3	9600	42.637	8200	42.464
1990 Mar 2.8	7953.3	9600	42.645	8300	42.467
1990 Mar 3.8	7954.3	9300	42.627	8000	42.461
1990 Mar 7.8	7958.3	8100	42.581	7100	42.439
1990 Mar 8.8	7959.3	8200	42.582	7200	42.441
1990 Mar 22.8	7973.3	6700	42.444	6000	42.334
1990 Jun 21.4	8063.9	—	41.892	—	41.798
1990 Jun 25.4	8067.9	—	41.778	—	41.621
1990 Jun 29.4	8071.9	—	41.661	—	41.568
1990 Jul 4.4	8076.9	—	41.443	—	41.349
1990 Jun 12.4	8084.9	—	41.412	—	41.319
1990 Aug 1.4	8104.9	—	41.335	—	41.242
1990 Aug 12.4	8115.9	—	41.270	—	41.180
1990 Aug 24.4	8127.9	—	41.251	—	41.158
1990 Sep 15.3	8149.8	—	41.183	—	41.089
1990 Oct 10.2	8174.7	—	41.085	—	40.992
1990 Oct 14.2	8178.7	—	41.088	—	40.995
1990 Oct 20.3	8184.8	—	41.028	—	40.936
1990 Oct 24.3	8188.8	—	41.003	—	40.911
1990 Nov 9.3	8204.8	—	40.936	—	40.843
1990 Dec 11.2	8236.7	—	40.880	—	40.787
1990 Dec 19.2	8244.7	—	40.798	—	40.705
1990 Jan 10.1	8266.6	—	40.752	—	40.659
1991 Jan 16.1	8272.6	—	40.754	—	40.661

[a] assuming A_V = 1.5
[b] assuming distance to NGC 1035 of 21 Mpc
[c] assuming A_V = 1.2

that supernovae reach bolometric maximum at shock break out. Comparison of the bolometric light curves show that the plateau phase of SN 1990E lasted approximately 25 days longer than that of SN 1987A. After the plateau, the bolometric luminosity of SN 1990E decreased dramatically for two weeks, and then declined exponentially until the supernova faded beyond detection with an *e*-folding time of 120 ± 10 days.

The observed exponential decline is slightly slower, but not significantly different from, the 105 day *e*-folding time observed for SN 1987A (Whitelock *et al.* 1988; Bouchet *et al.* 1991). Models of SNe II suggest the exponential tail of the light curve is powered by the decay of ^{56}Co, with *e*-folding time of 111.3 days, and our observations are consistent with these results. An additional constant energy source, such as a pulsar, would cause the exponential decline to have an *e*-folding time longer than that of ^{56}Co. From our photometric observations of SN 1990E, we derive an upper limit of $7\times10^{39}(D/21\ \mathrm{Mpc})^2$ ergs s^{-1} for the contribution to the optical and infrared luminosity of a pulsar or accreting neutron star within the forming remnant of SN 1990E. This is substantially larger than the optical-IR luminosity seen from the Crab Nebula, 2×10^{37} ergs s^{-1} (Kirshner 1974) and the current upper limit for SN 1987A (8×10^{36} ergs s^{-1}; Suntzeff *et al.* 1992).

The observed flux during the exponential decline of the bolometric light curve can be used to determine the amount of ^{56}Ni, the parent nucleus of ^{56}Co, produced in the explosion of SN 1990E. We assume that all energy released in the decay of ^{56}Co, except that associated with neutrinos, is deposited into the surrounding material. For SN 1990E this is a reasonable assumption because the observed rate of decline matches the decay rate of ^{56}Co. If a substantial fraction of the gamma rays produced in radioactive decay were leaking out of the SN, we would expect the exponential rate of decline to be faster than 111.3 days, because the optical depth for the gamma rays decreases as the SN expands. The average decay energy for ^{56}Co, including the effect of neutrino losses, is 3.695 MeV/decay (Woosley *et al.* 1989). If we take the explosion date for SN 1990E to be JD=2447932 and assume that the average ^{56}Co nucleus was formed 9 days later (the *e*-folding time of ^{56}Ni, the parent nucleus of ^{56}Co), we find the amount of nickel produced in the explosion of SN 1990E to be

$$\mathcal{M}(^{56}\mathrm{Ni}) = 0.073\mathcal{M}_\odot\left(\frac{D}{21\ \mathrm{Mpc}}\right)^2 10^{0.8[(A_v-1.5)/2.5]}. \quad (3)$$

Given the uncertainty in extinction and distances discussed above, we estimate the nickel mass to be $0.022 < \mathcal{M}(^{56}\mathrm{Ni}) < 0.091\ \mathcal{M}_\odot$. The nickel mass for SN 1987A was determined to be $0.071^{+0.019}_{-0.016}\mathcal{M}_\odot$ (Suntzeff & Bouchet 1990), and consequently the amount of nickel produced by SN 1990E is roughly equivalent to that produced in SN 1987A. Phillips *et al.* (1990) show that the absolute *B* and *V* magnitudes at late times of SN 1983K and SN 1969L, using $H_0=75$ km s^{-1} Mpc^{-1}, are similar to that of SN 1987A and hypothesize that most SNe II-P events produce equal amounts of ^{56}Ni. If we chose a distance to SN 1990E corresponding to $H_0=75$ km s^{-1} Mpc^{-1}, we would find that SN 1990E ejected half the nickel of the SNe studied by Phillips *et al.* However, because of the large photometric errors and uncertainties in the distances, our data for SN 1990E are still consistent with their hypothesis. At present, the amount of ^{56}Ni produced in SNe II explosion models is a free parameter except for 20 $\mathcal{M}_\odot$ stars, which are constrained by the observations of SN 1987A (Thielemann *et al.* 1992). Similar determinations of the nickel mass ejected in other SNe II explosions would constrain explosion models for other SNe II progenitors and would be of considerable use.

5. CONCLUSIONS

SN 1990E is one of the few SNe II-P which has been well observed before maximum brightness. Images taken of NGC 1035 five days before the discovery of SN 1990E with the BASST Telescope show that the SN brightened by more than a magnitude in *R* during this time period. The rapid rise in its light curve, coupled with an estimate of the SN's age using the Expanding Photosphere Method, lead us to believe that the SN was very young at discovery and that typical SNe II-P reach *B* maximum within 2 weeks of core collapse. In addition, our unique *J* and *H* light curves demonstrate that the rise to maximum is protracted at longer wavelengths.

The early time spectral observations of SN 1990E provide the first high signal-to-noise ratio observations of a typical SNe II-P while it was extremely hot, and these observations have enabled us to identify several N II lines. The spectral and photometric evolution of SN 1990E is similar to other *typical* SNe II-P such as SN 1969L through the photospheric phase, but is much slower than SN 1987A; this behavior suggests that SN 1990E resulted from the explosion of a red supergiant. Additional support for the progenitor being a red supergiant may be provided by the observation of N II lines. These lines, which were not seen in the earliest spectra of SN 1987A, may indicate some enhancement of nitrogen in the outer regions of SN 1990E's progenitor, something expected in red supergiants.

Images show that SN 1990E occurred near an unresolved H II region in the disk of its highly inclined host galaxy. In addition, the spectra show strong Na D absorption at the recession velocity of NGC 1035 and a relatively red continuum even at early times when high ionization lines are present. These observations lead us to believe that SN 1990E is significantly affected by extinction from interstellar dust in its host galaxy. We estimate the extinction to the SN to be $A_V=1.5\pm0.3$ mag by comparing its colors to SN 1987A at epochs when the He I λ5876 line is last seen. Because the strength of most lines in SNe atmospheres is primarily temperature dependent, this method can be applied to nearly all SNe II and could be used with other lines such as Si II λ6355 or Fe II λ5169. The effectiveness of this method will be more fully realized when *BVRI* photometry and spectra are available for other SNe II that are not reddened. Atmospheric models that treat the line-forming elements in non-LTE could also eliminate much of the uncertainty.

From the photometry we have constructed a bolometric light curve. Even at the time of discovery, the bolometric luminosity of SN 1990E was falling rapidly. Given the youth of the SN at this time, it appears that the bolometric maximum probably occurred near shock breakout. In the nebular phase, the bolometric luminosity of SN 1990E declined at a rate equal (within the uncertainties) to the radioactive decay rate of ^{56}Co. Because the decline is essentially equal to ^{56}Co's decay rate, we expect that nearly all of the gamma rays produced by the decay of this nucleus were thermalized and powered the SN after the fall from the plateau. With these conclusions, we use the bolometric light curve to estimate that SN 1990E produced $0.073^{+0.018}_{-0.051}\mathcal{M}_{\odot}$ of ^{56}Ni, an amount virtually identical to SN 1987A.

This data set will provide the basis for a detailed study of the atmospheres of SNe resulting from red supergiants (Eastman *et al.* 1993). With this study we hope to evaluate the accuracy of SNe II explosion models, estimate the mass of the SN 1990E's progenitor, and determine the abundances of several elements (e.g., nitrogen). In addition, these models will provide an estimate of SN 1990E's luminosity as a function of time and will enable the determination of its distance in a way completely independent of all steps of the cosmic distance ladder.

We would like to thank J. Halpern, W. Sargent, J. Raymond, and R. Green for contributing data to this paper. We are grateful to R. Eastman, P. Pinto, and F. K. Thielemann for sharing their insights on SNe II-P. Supernova research at the Harvard University is supported by NSF Grant No. AST 89-05529 and NASA Grant Nos. NAG 5-841 and NGT-51002. A.V.F acknowledges the support of NSF Grant Nos. AST-8957063 and AST-9115174, as well as NSF Cooperative Agreement AST-8809616 (Center for Particle Astrophysics, U. C. Berkeley). Construction of the SONIC was supported by the Scholarly Studies Fund of the Smithsonian Institution.

REFERENCES

Aaronson, M., Bothun, G., Cornell, M. E., Huchra, J. P., & Schommer, R. A. 1986, ApJ, 302, 536
Arnett, W. D., Bahcall, J. N., Kirshner, R. P., & Woosley, S. E. 1989, ARA&A, 27, 629
Barbon, R., Ciatti, F., & Rosino, L. 1979, A&A, 72, 287
Barbon, R., Ciatti, F., & Rosino, L. 1982a, A&A, 116, 35
Barbon, R., Ciatti, F., & Rosino, L., Ortolani, S., & Rafanelli, P. 1982b, A&A, 116, 43
Benetti, S., Cappellaro, E., & Turatto, M. 1990, IAU Circular, No. 4977
Bessell, M. S. 1990, PASP, 102, 1181
Blanco, V. M., *et al.* 1987, ApJ, 320, 589
Bouchet, P., Phillips, M. M., Suntzeff, N. B., Gouiffes, C., Hanuschik, R. W., & Wooden, D. H. 1991, A&A, 245, 490
Branch, D. 1987, ApJ, 320, L121
Branch, D. 1990, in A&A Library: Supernovae, edited by A. G. Petschek (Springer, New York), p. 30
Burstein, D., & Heiles, C. 1984, ApJS, 54, 33
Chugai, N. N. 1982, Astron. Zh., 59, 1134
Chugai, N. N. 1988, Ap&SS, 146, 375
Ciatti, F., Rosino, L., & Bertola, F. 1971, MSAIt, 41, 163
Cousins, A. W. J. 1980, S. Afr. Astron. Obs. Circ., 1, 116.
Cousins, A. W. J. 1981, S. Afr. Astron. Obs. Circ., 6, 4
de Vaucouleurs, G., de Vaucouleurs, A., Buta, R., Ables, H. D., & Hewitt, A. V. 1981, PASP, 93, 36
Dwek, E. 1990, ApJ, 329, 814
Dwek, E., *et al.* 1983, ApJ, 274, 168
Dwek, E. 1983, ApJ, 274, 175
Eastman, R. G., & Kirshner, R. P. 1989, ApJ, 347, 771
Eastman, R. G., Schmidt, B. P., & Kirshner, R. P. 1993, ApJ (to be submitted)
Filippenko, A. V., Porter, A. C., Sargent, W. L. W., & Schneider, D. P. 1986, AJ, 92, 1341
Filippenko, A. V., & Sargent, W. L. W. 1986, AJ, 91, 691
Filippenko, A. V. 1992, ApJ, 384, L37
Freedman, W. L. 1990, ApJ, 355, L35
Graham, J. A. 1982, PASP, 94, 244
Hamuy, M., Suntzeff, N. B., Gonzales, R., & Martin, G. 1988, AJ, 95, 63
Harris, W. E., Fitzgerald, M. P., & Reed, B. C. 1981, PASP, 93, 507
Hayes, D. S., Latham, D. W., & Hayes, S. H. 1975, ApJ, 197, 587
Johnson, H. L., Mitchell, R. I., Iriarte, B., & Wisniewski, W. Z. 1966, Commun. Lunar Plant. Lab, 4, 99 (JMIW)
Johnson, H. L., & Morgan, W. W. 1953, ApJ, 117, 313
Kirshner, R. P. 1974, ApJ, 194, 323
Kirshner, R. P. 1990, in A&A Library: Supernovae, edited by A. G. Petschek (Springer, New York), p. 59
Kirshner, R. P., & Kwan, J. 1974, ApJ, 193, 27
Kirshner, R. P., Oke, J. B., Penston, M. V., & Searle, L. 1973, ApJ, 185, 303
Landolt, A. U. 1983, AJ, 88, 439
Landolt, A. U. 1992, AJ, 104, 340
Leibundgut, B., Kirshner, R. P., Pinto, P. A., Rupen, M. P., Smith, R. C., Gunn, J. E., & Schneider, D. P. 1991, ApJ, 372, 521
Lopez, R. 1990, IAU Circular, No. 5131
Lopez, R., & Gomez, G. 1991 IAU Circular, No. 5174
Lopez, R., Rodriguez, J. A., Balcells, M., & Cepa, J. 1990, IAU Circular, No. 5078
Mateo, M., & Schechter, P. L. 1989, in The First ESO/ST-ECF Data Analysis Workshop, edited by P. J. Grosbol, F. Murtagh, and R. H. Warmels (ESO, Garching), p. 69.
Menzies, J. W., *et al.* 1987, MNRAS, 227, 39P
Merrill, P. W. 1958, Lines of the Chemical Elements in Astronomical Spectra (Carnegie Institution of Washington), Publication 610
Nomoto, K., Filippenko, A. V., & Shigeyama, T. 1990, A&A, 240, L1
Pennypacker, C., & Perlmutter, S. 1990, IAU Circular, No. 4965
Perlmutter, S., Crawford, F. S., Muller, R. A., Pennypacker, C. R., Sasseen, T. P., Smith, C. K., Treffers, R., & Williams, R. 1988, in Instrumentation for Ground-Based Optical Astronomy, edited by L. B. Robinson (Springer, New York), p. 674
Phillips, M. M., Hamuy, M., Maza, J., Ruiz, M-T., Carney, B. W., & Graham, J. A. 1990, PASP, 102, 299
Phillips, M. M., Heathcote, S. R., Hamuy, M., & Navarette, M. 1988, AJ, 95, 1087
Sandage, A., & Tammann, G. 1981, Revised Shapley–Ames Catalog of Galaxies (Carnegie Institution of Washington)
Schlegel, E. M., & Kirshner, R. P. 1989, AJ, 98, 577
Schmidt, B. P., Kirshner, R. P., & Eastman, R. G. 1992, ApJ, 395, 366
Schmutz, W., Abbot, D. C., Russell, R. S., Hamann, W. R., & Wessolowski, U. 1990, ApJ, 355, 255
Suntzeff, N. B., & Bouchet, P. 1990, AJ, 99, 650
Suntzeff, N. B., *et al.* 1992. ApJ, 384, L33
Thielemann, F-K., Nomoto, K., & Hashimoto, M. 1992, preprint
Uomoto, A. 1986, ApJ, 310, L15
Uomoto, A., & Kirshner, R. P. 1986, ApJ, 388, 685

Whitelock, P. A., *et al.* 1988, MNRAS, 234, 5P
Whitford, A. E. 1958, AJ 63, 201
Williams, R. E. 1987, ApJ, 320, L117
Woosley, S. E., Pinto, P. A., & Hartman, D. 1989, ApJ, 346, 393
Woosley, S. E., Pinto, P. A., Martin, P. G., & Weaver, T. A. 1987, ApJ, 318, 664
Woosley, S. E., & Weaver, T. A. 1986, ARA&A, 24, 205
Young, T. R., & Branch, D. 1989, ApJ, 342, L79

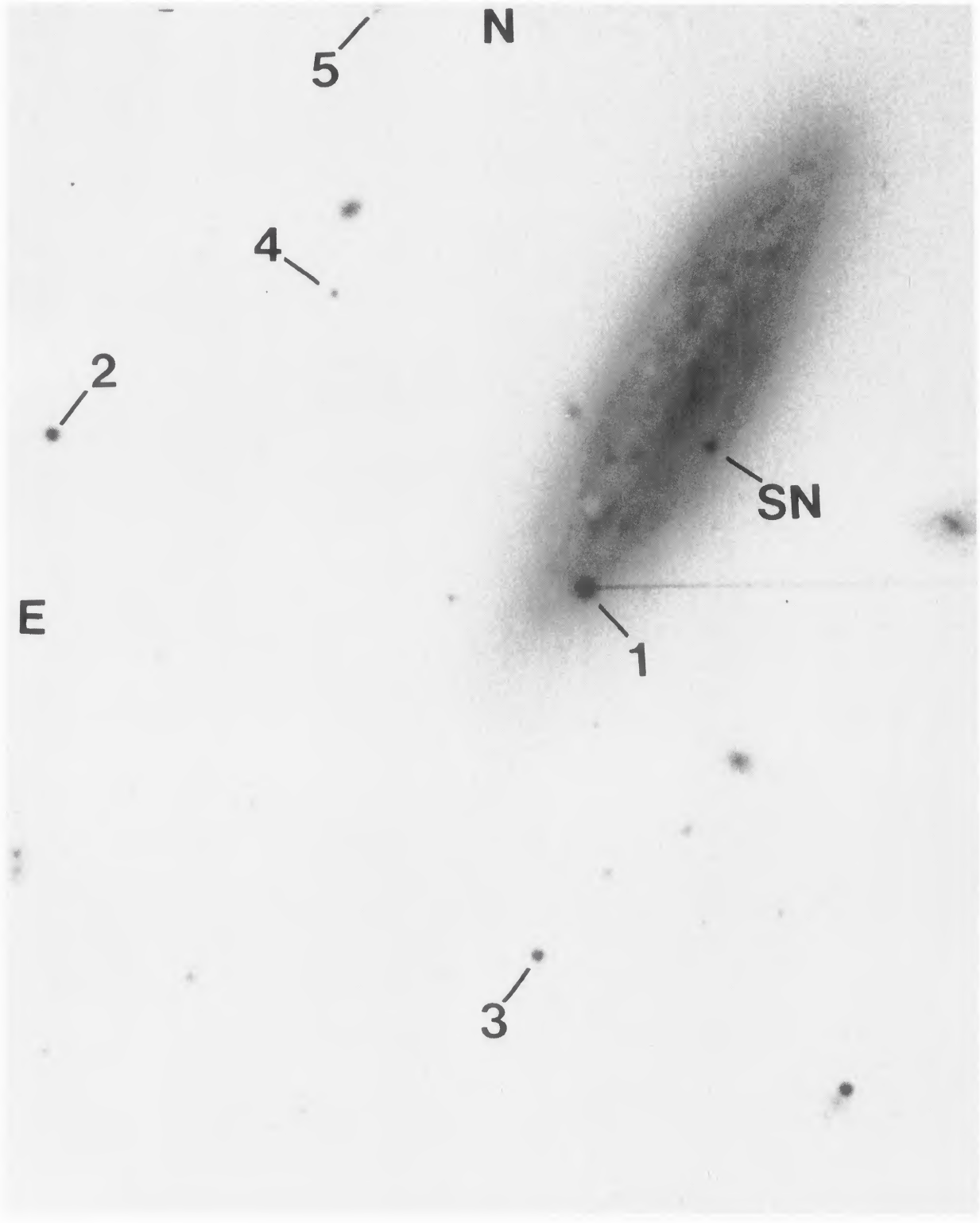

FIG. 1. *R* CCD image taken with the CTIO 0.91 m telescope showing the location of the SN 1990E and the field reference stars.

Schmidt *et al.* (see page 2238)